

Spherical Mass Distribution Formalism

With Application for Gravitational Simulations

Rod Luhn

Updated 5/31/2023

Original Date 5/4/2008

This document presents formalism for using spherically symmetric mass distributions and applications for gravitational many-body simulations. I present a sampling of distribution candidates for use in my simulation code. Finally, I have presented for my own reference, how to ultimately extract mass density functions from simulation data that can be compared to a density model using the included formalism. In addition, I have presented how to use this formalism to create density functions to compare with mass densities extracted from simulation results for my simulation studies.

Contents

- 1 Spherically Symmetric Mass Distributions..... 3
- 2 Significance of M(R) 3
- 3 Introduction to the Mass Distribution Formalism 3
- 4 Detailed Look at distributions..... 6
 - 4.1 Exponential Functions..... 7
 - 4.1.1 When m=0..... 7
 - 4.1.1.1 When m=0 and $\alpha=3/n$ 8
 - 4.1.1.2 When m=0 and $\alpha=2$, the Gaussian Form (Added 10/7/2019) 10
 - 4.1.1.3 When m=0 and $\alpha=2/3$ (added 5/15/2016) 10
 - 4.1.1.4 When m=0 and $\alpha=5/6$ (added 7/25/2016) 10
 - 4.1.2 When m=1..... 11
 - 4.1.2.1 When m=1 and $\alpha=2/n$ (added 5/31/2023) 11
 - 4.1.3 When m=2..... 12
 - 4.2 Functions using powers of distance..... 13
 - 4.2.1 $F(x)=1$ 13
 - 4.2.2 $F(x)=1-x$ 14
 - 4.2.3 $F(x)=(1-x)^2$ 14
 - 4.2.4 $F(x)=(1-x)^4$ 15
 - 4.2.5 $F(x)=1-x^2$ 15
 - 4.3 Other Power Law Forms 16
 - 4.3.1 $FX(0:3:1)$ 16
 - 4.3.2 $FX(0:3:p)$ (added 12/30/2013) 17
 - 4.3.3 $FX(-1:4:p)$ (added 1/8/2013) 18
 - 4.3.4 Plummer’s Model, $FX(0:2:1.5)$ (added 3/16/2016)..... 18
 - 4.3.5 General Plummer Model $FX(0:p:1/p)$ (added 3/20/2016)..... 19
 - 4.3.6 NFW(M) Density Profile: $FX(1:1:1)$ (added 8/24/2018) 20
 - 4.3.6.1 Practical Solution for Scaling Constant from Simulation Density Profile..... 21
 - 4.3.7 Jaffe Profile (Extended) : $FX(2,1,p)$ (added 8/24/2018)..... 22
 - 4.3.8 $FX(1.5,1,1)$ (added 11/26/2022)..... 23
- 5 Notes on Using the Density Functions..... 23

5.1	Comparing Simulation Data to the Density Model	23
5.2	Reconstructing the Density Function from the Mass Function	26
5.3	Poisson Equation and the relation between the Density and $M(R)$ (Added 2/24/2017)	26
6	Using This Formalism (Added 5/15/2016)	28
6.1	About the Simulation Data.....	28
6.2	Modeling the Mass Distribution Data.....	32
6.3	Mass Density Analysis Results.....	32
7	Conclusions	36

1 Spherically Symmetric Mass Distributions

This investigation of mass distributions is intended to provide a connection to collections of gravitating systems of small objects. It is a simplistic study of spherically symmetric mass distributions for the purpose of how and if they might be used in my gravitational simulation. To be useful for computational purposes, simplicity and some semblance of reality in modeling real systems are the most important qualities.

2 Significance of M(R)

The motivation for this analysis stems from the need in my simulation to use simple mass distributions for some or all of the simulation objects. When using spherical mass distributions, it is important to be able to determine the mass inside a radius R of a distribution. Below I use the term M(R) for this mass quantity. Why is M(R) important?

Gauss' law from electrodynamics describes the behavior of a test particle inside a spherical charge distribution. It is shown that the test particle is only affected by the charge contained within the charge distribution at the test particle distance R. Note that both gravitational mass and electric charge distributions share this same property and so one might be able to model a moving object within a mass distribution by using this Gauss' law property. If one can model how much mass is inside the distribution and know the current position of a test particle, one can determine the force on that moving object based on M(R).

In addition to the above, M(R) is easily extracted from my simulation data and using the formalism below one can extract an analytical representation of the mass density as it evolves in the context of the simulation.

3 Introduction to the Mass Distribution Formalism

I began thinking about spherical mass distributions and over time the following formalism evolved as being the most useful for evaluation and suitability to the simulation. A mass density function¹ $\rho(r)$ represents a spherically symmetric collection of mass, where if integrated from $r=0$ to ∞ , will give the total mass of the distribution M_T . Suppose this mass distribution is composed of a superposition of several (say N in total) mass distributions, we can write the total mass distribution as:

Equation 1

$$\rho(r) = \sum_{i=1}^N \rho_i(r)$$

¹ I have succumbed to "peer" pressure in the symbol used for the density function. It is clear from literature and from past physics training that the Greek letter rho is used for density functions. I now use that symbol in my document.

$$M_T = \int \rho(r) d^3r = \int \sum_{i=1}^N \rho_i(r) d^3r = \sum_{i=1}^N \int \rho_i(r) d^3r = \sum_{i=1}^N M_{Ti}$$

Where M_{Ti} is the total mass contribution of each of the separate mass distributions to the total mass. The above integral, when integrated out to specific distance, "R", gives the total mass inside radius R, which is the $M(R)$ quantity discussed above. This integral is seen below:

Equation 2

$$M(R) = \int_0^R \rho(r) d^3r = \sum_{i=1}^N \int_{r=0}^{r=R} \rho_i(r) d^3r$$

Or we can write the individual distribution integrals as:

$$M_i(R) = \int_0^R \rho_i(r) d^3r$$

Since these integrals are spherically symmetric, the angular solutions are easy and thus picking a distribution that is interesting and integrable becomes the challenge.

The purpose of this study is look at what might give realistic results for gravitating systems, so that they may be included into the **Riod** simulation. In that light, I want to simplify the above equations based on a simple scaling of the distribution. For the total mass integral for the i_{th} distribution becomes:

Equation 3

$$M_{Ti} = \int_0^{2\pi} d\phi \int_0^\pi d\theta \sin\theta \int_0^\infty r^2 \rho_i(r) dr$$

$$M_i(R) = \int_0^{2\pi} d\phi \int_0^\pi d\theta \sin\theta \int_0^R r^2 \rho_i(r) dr$$

It is convenient to let the density function, ρ_i be composed of a density scaling constant A_i and a function that holds the distance component. Let's use the following:

$$\rho_i(r) = A_i f_i(r)$$

Note that we chose $f_i(r)$ to be a unitless function of r where all instances of distance are scaled by a distance constant as shown below. This choice puts all the units into the A_i constant.

The angular integrals are a known result and are equal to 4π . Thus, with the angular integrals performed in Equation 3, we get:

$$M_{Ti} = 4\pi A_i \int_0^{\infty} f_i(r) r^2 dr$$

$$M_i(R) = 4\pi A_i \int_0^R f_i(r) r^2 dr$$

We now chose to scale the integrals by a distance scaling constant, so that the integrals become more simple functions of that scaling and the distance. We substitute $x=r/a_i$ or $r=xa_i$ and $dr=a_i dx$ into the above integrals and after making the appropriate changes to the integral and we get the total distribution mass and mass at R integrals as in Equation 4.

Equation 4

$$M_{Ti} = 4\pi a_i^3 A_i \int_0^{\infty} x^2 f_i(x) dx$$

$$M_i(R) = 4\pi a_i^3 A_i \int_0^{R/a_i} x^2 f_i(x) dx$$

Once $f(x)$ is known and the integral for M_{Ti} is computed, the value is just a unitless number that we will call β_i . Thus:

$$\beta_i = \int_0^{\infty} x^2 f_i(x) dx$$

And,

$$M_{Ti} = 4\pi a_i^3 A_i \beta_i$$

Or A_i is defined as:

$$A_i = M_{Ti} / 4\pi a_i^3 \beta_i$$

Note A_i has units of mass per unit volume as a mass density should. Now if we use the above result in Equation 4, we can rewrite it in the following form:

Equation 5

$$M_i(R) = 4\pi a_i^3 A_i \int_0^{R/a_i} x^2 f_i(x) dx = \frac{M_{Ti}}{\beta_i} \int_0^{R/a_i} x^2 f_i(x) dx$$

Because $M(R)$ is really just a function of the ratio $R/a_i \equiv z_i$ we will use the following constructs to discuss the mass ratio at R as the function $g_i(z_i)$ which we will call the Mass Distribution Ratio as the following:

Equation 6

$$g_i(z_i) = \frac{M_i(R)}{M_{Ti}} = \frac{1}{\beta_i} \int_0^{z_i} f_i(x) x^2 dx$$

And so, the mass at distance R for the i_{th} distribution can be written:

$$M_i(R) = M_{Ti} g_i(z_i) = M_{Ti} g_i(R/a_i)$$

The total mass at R from all the distributions in the superposition can be written:

Equation 7

$$M(R) = \sum_{i=1}^N M_{Ti} g_i(z_i) = \sum_{i=1}^N M_{Ti} g_i(R/a_i)$$

Note that $g_i(z_i)$ is a normalized distribution function that, when $f(x)$ is well behaved, is bounded when $z=0$, $g=0$ and when $z=\infty$, $g=1$. Note too that $g_i(z_i)$ is the mass ratio of the accumulated mass at distance R to the total mass of that distribution. This is convenient to use this form when we are talking about a single distribution, $N=1$ in the above formalism.

Another convenient form for Equation 7 is the following:

$$M(R) = M_T \sum_{i=1}^N \frac{M_{Ti}}{M_T} g_i(R/a_i)$$

Or:

Equation 8

$$\frac{M(R)}{M_T} = \sum_{i=1}^N \frac{M_{Ti}}{M_T} g_i(R/a_i)$$

Note that quantity $M(R)/M_T$ in Equation 8 is easily extracted from simulation data and that choosing specific Mass Ratio Distributions, $g_i(R/a_i)$, one can create a model for the mass distribution from simulation data. See Section 6 for an example of how this is done.

4 Detailed Look at distributions

Using the above formalism, we can determine specific mass distribution properties from integrable functions $f(x)$. Note, in the discussion that follows we will be looking at individual distributions and thus drop the “ i ” index since N will be 1 from the above. Note too that once we determine $g(z)$, it can be used in the above for more complex mass distributions.

What are the important properties for potential $f(x)$? Considerations for $f(x)$ are listed below:

1. It must be a dimensionless quantity and thus all values of radial distance “ r ” must be scaled with our constant “ a ”.

2. It must be bounded at large distances to be either zero or vanishingly small.
3. It must be finite at $x=0$.
4. It must be integrable across from $x=0$ to $x=\infty$ (or to the extent of the distribution).
5. The resulting distribution should be computationally simple to use in my simulation code.

Below we will examine several types of distributions that fit the above criteria.

4.1 Exponential Functions

Exponential functions are interesting since they are bounded and as we shall see many are integrable. Since the integrals contain powers of x , a generalization of the function will include terms with other powers of x . In this generalized case we write the density function as:

Equation 9

$$f(x) = x^m e^{-x^\alpha} \text{ and thus } \beta = \int_0^\infty x^{m+2} e^{-x^\alpha} dx ; m \geq 0 \text{ and } \alpha > 0 .$$

Note that for now, m is restricted to integers but α is just a positive number. The mass at distance integral is:

$$M(R) = \frac{M_T}{\beta} \int_0^{\frac{R}{a}} x^{m+2} e^{-x^\alpha} dx .$$

And the mass fraction is:

$$g(z) = \frac{M(R)}{M_T} = \frac{1}{\beta} \int_0^{\frac{R}{a}} x^{m+2} e^{-x^\alpha} dx \text{ where } z = R/a.$$

These functions will be examined below for special cases of m and α .

4.1.1 When $m=0$

Perhaps the simplest and most interesting variant of these exponential functions to start with is when using $m=0$ in Equation 9. We can write the mass fraction as a function of the dimensionless parameter $z=R/a$;

$$g(z) = \frac{1}{\beta} \int_0^z x^2 f(x) dx = \frac{1}{\beta} \int_0^z x^2 e^{-x^\alpha} dx$$

One recognizes this function is commonly used in the astrophysical journals as the Einasto density profile. In those cases, α takes values on the order of $\frac{1}{4}$ and smaller. Using the method that follows, I have implemented values of $\frac{1}{4}$, $1/6$, and $1/7$ for the comparisons with density profile data.

4.1.1.1 When $m=0$ and $\alpha=3/n$

Let's look at a class of functions where again $m=0$ and $\alpha=3/n$, where n is a positive integer greater than zero. Note that the Einasto forms mentioned above are variants of this form as $3/12$, $3/18$ and $3/21$ and the fractions used. However, the solutions of these variants are cumbersome to say the least, especially for spreadsheet use.

Let's first look at $n=3$, and note that this is just a simple exponential function:

This can be written as a ratio of the mass at distance to the total mass, $M(R)/M_T$. We will also use the unitless value $z=R/a$. Thus we have;

$$g(z) = \frac{M(z)}{M_T} = 1 - e^{-z} \left(\frac{z^2}{2} + z + 1 \right)$$

The Taylor series expansion for $g(z)$ near $z=0$ is :

$$g(z) = \frac{z^3}{6} - \frac{z^4}{8} + \frac{z^5}{20} - \dots$$

This distribution of mass seems odd at first since there is no appreciable mass at $z=0$ since $M_R(z)$ increases with z cubed. Given that this is an exponential function, the most mass is concentrated near $R=0$ but because of the three dimensional integral, the mass doesn't accumulate to 50% of the total until $Z \cong 2.7$. We will see that this behavior is mirrored in all the distributions examined below.

This is an important distribution for another reason. It is the only one in the series ($m=0$) where the behavior near $R=0$ goes as R^3 . Based on simulation results, this is an important behavior since one might think that most real matter distributions to resemble a uniform distribution near $R=0$ and uniform distributions have that R^3 behavior near $R=0$.

For this function, $\beta=1/2$ and $R_v/a=3.205$ and $g(z=R_v)=0.6211$

Examining this functional form for $n=1$ we have $\beta=1/3$ and the integral's solution for the mass fraction is the following:

$$g(z) = 1 - e^{-z^3}$$

This form is important because it is the localized force softening form that is used in the Riod gravitational simulation. The Taylor series expansion for $g(z)$ near $z=0$ is :

$$g(z) = \frac{z^3}{1} - \frac{z^6}{2} + \frac{z^9}{6} - \dots$$

For other n , let us reduce the equation's writing complexity by setting $X=z^{3/n}$, we provide the following list:

For $n=2$, $X=z^{3/2}$, $\beta=2/3$: $g(z) = 1 - e^{-X}(X + 1)$

For $n=3$, this is the result we saw above, where $X=z^{3/3}$, $\beta=2$ and: $g(z) = 1 - e^{-X} \left(\frac{X^2}{2} + X + 1 \right)$

For $n=4$, $X=z^{3/4}$ $\beta=8$ and $g(z) = 1 - e^{-X} \left(\frac{X^3}{6} + \frac{X^2}{2} + X + 1 \right)$

For $n=5$, $X=z^{3/5}$ $\beta=40$ and $g(z) = 1 - e^{-X} \left(\frac{X^4}{24} + \frac{X^3}{6} + \frac{X^2}{2} + X + 1 \right)$

For $n=6$, $X=z^{3/6}$ $\beta=240$ and $g(z) = 1 - e^{-X} \left(\frac{X^5}{120} + \frac{X^4}{24} + \frac{X^3}{6} + \frac{X^2}{2} + X + 1 \right)$

For $n=7$, $X=z^{3/7}$ $\beta=1680$ and $g(z) = 1 - e^{-X} \left(\frac{X^6}{720} + \frac{X^5}{120} + \frac{X^4}{24} + \frac{X^3}{6} + \frac{X^2}{2} + X + 1 \right)$

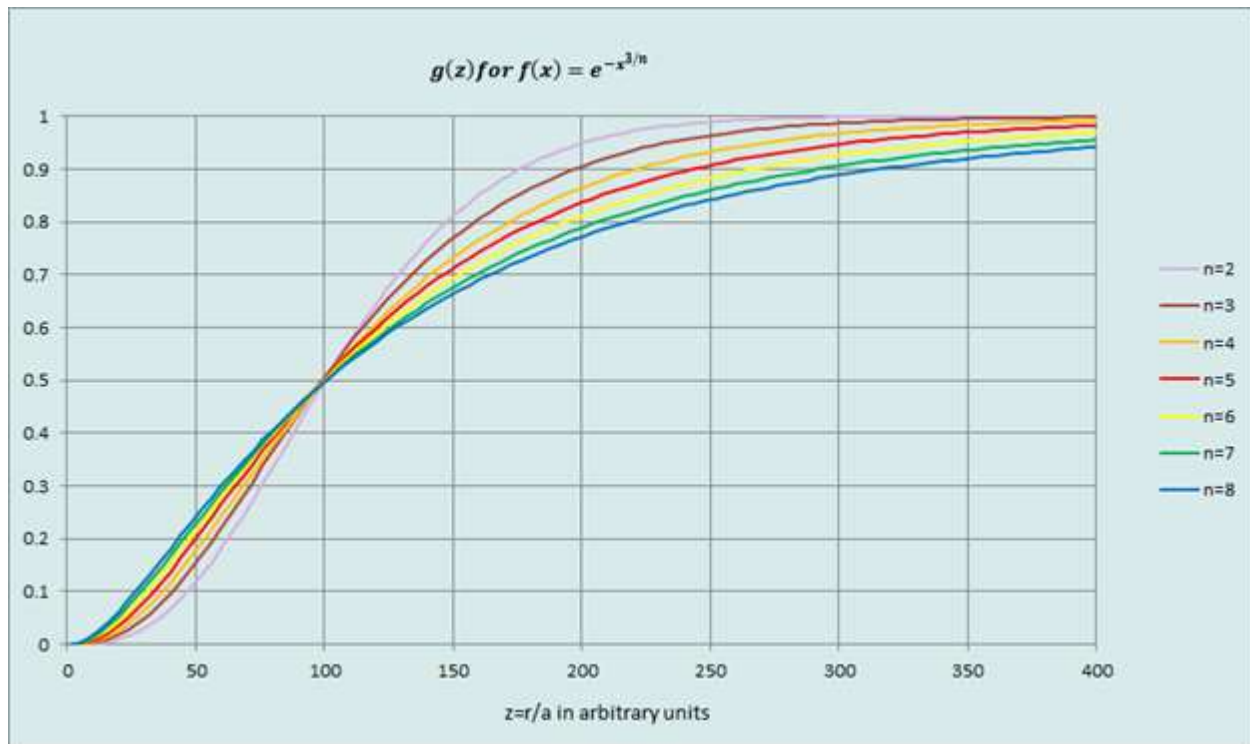
One can see a pattern here, and in general the solution is, $\beta=n!/3$:

$$g(z) = 1 - e^{-X} \sum_{i=0}^{n-1} \frac{X^i}{i!}$$

And the Taylor series expansion near $z=0$ looks like the following, note $g(z) \sim z^3$ for all these functions:

$$g(z) = \frac{z^3}{n!} + O(z^{(3n+3)/n}) \dots$$

A plot of the behavior of these functions is seen below (all curves adjusted to have $g(100) \approx 0.5$):



Of note in the above figure is that as n increases, the tail of the distribution is extended and the behavior at $g(z)=0.1$, z moves smaller values. The importance of this behavior is that this is similar to what

happens in my simulation as a gravitating gas ball evolves in time. I may use these functions in my analysis of the gas ball simulations.

For this function and $n=1$, the $R_v/a=0.9989$ and $g(z=R_v)=0.6309$

For this function and $n=2$, the $R_v/a=1.6656$ and $g(z=R_v)=0.6281$

For this function and $n=3$, the $R_v/a=3.2036$ and $g(z=R_v)=0.6209$

For this function and $n=4$ the $R_v/a=6.871$ and $g(z=R_v)=0.6130$

4.1.1.2 When $m=0$ and $\alpha=2$, the Gaussian Form (Added 10/7/2019)

The Gaussian form is one of interest and I didn't include it initially since the solution requires the ERF function and I didn't know that there are standard implementations of this included in Excel and GNU FORTRAN until I looked for them specifically.

I have included this as a new option in the RIOD simulation. The function is:

$$f(x) = e^{-x^2}$$

For this function, $\beta = \pi^{0.5}/4$ and the mass ration function is:

$$g(z) = \text{ERF}(z) - \frac{2ze^{-z^2}}{\sqrt{\pi}}$$

For this function, the $R_v/a=1.2547$ and $g(z=R_v)=0.6307$

4.1.1.3 When $m=0$ and $\alpha=2/3$ (added 5/15/2016)

Another interesting variant is the following:

$$f(x) = e^{-x^{2/3}} \text{ and } M(R) = \frac{M_T}{\beta} \int_0^{R/a} x^2 e^{-x^{2/3}} dx$$

This form factor for the mass density has a $\beta=315 \pi^{1/2}/32$ and the mass fraction function is:

$$g(z) = \text{erf}(\sqrt[3]{z}) - \frac{2 e^{-z^{2/3}} \sqrt[3]{z} \{8 z^7 + 28 z^5 + 70 z^3 + 105 z\}}{105 \sqrt{\pi}}$$

I include this one because it fits snugly between some of the other variants above and Excel spreadsheets and my FORTRAN compiler have the ERF(X) function built in. I have trialed this function in spreadsheets but has not made it into the FITS.EXE program as of yet.

4.1.1.4 When $m=0$ and $\alpha=5/6$ (added 7/25/2016)

A variant of the above is one where the exponent of x is greater than 1. Functions of this type are of interest for modeling mass distributions because they peaked near the origin but will poll over at the peak rather than form a stronger peak.

$$f(x) = e^{-x^{6/5}} \text{ and } M(R) = \frac{M_T}{\beta} \int_0^{R/a} x^2 e^{-x^{6/5}} dx$$

The solution for $g(z)$ is similar to the above function where $\beta=5 \pi^{1/2}/8$ and the mass ratio function is:

$$g(z) = \text{erf}(z^{3/5}) - \frac{2 e^{-z^{6/5}} z^{3/5} \{2z^{6/5} + 3\}}{3 \sqrt{\pi}}$$

I have trialed this function in spreadsheets and while it looks to be a function of interest, it has not be coded into the FITS.EXE program as of yet.

4.1.2 When $m=1$

This class of functions have become interesting in that they have proven to be useful in fitting $M(R)$ from simulation data. Simulation density profiles demonstrate a propensity to form what appears to be a uniform density in the interior of the distribution. What is more is that the functional forms used to fit the data that have a uniform interior ($\sim R^3$ behavior) do not do a good job replicating the seen interiors. As such, moving to functions that go as R^4 give a better interior representation of the simulation data.

4.1.2.1 When $m=1$ and $\alpha=2/n$ (added 5/31/2023)

If we set $m=1$ and $\alpha=2/n$, in Equation 9, a quick calculation for β yields a value of 6. The mass ratio becomes the following:

$$f(x) = x e^{-x^{2/n}} \text{ and } g(z) = \frac{1}{\beta} \int_0^z x^3 e^{-x^{2/n}} dx$$

The most obvious value to start with would be $n=2$, or the simple exponential. The solution becomes.

$$g(z) = 1 - e^{-z} \left(\frac{z^3}{6} + \frac{z^2}{2} + z + 1 \right)$$

The Taylor series expansion for $g(z)$ near $z=0$ is :

$$g(z) = \frac{z^4}{24} - \frac{z^5}{30} + \dots$$

Here we see similar behavior as the $m=0$ case where now the mass ratio increases as z to the fourth power. Clearly, as n increases, the computational difficulty of using this format will become problematic.

For this function, the $R_v/a=4,365$ and $g(z=R_v)=0.6344$

Let's examine other values of n .

For this function, $n=1$ we get $\beta=1/2$ and thus:

$$g(z) = 1 - e^{-z^2} \{z^2 + 1\} \text{ where } X = z^2$$

The Taylor series expansion for $g(z)$ near $z=0$ is :

$$g(z) = \frac{z^4}{2} - \frac{z^6}{3} + \frac{z^8}{8} - \dots$$

For n=2 we have: $\beta=6$ and

$$g(z) = 1 - e^{-X} \left(\frac{X^3}{6} + \frac{X^2}{2} + X + 1 \right) \text{ where } X = z^1$$

And for n=2 we have determined that, $R_v/a=4,365$ and $g(z=R_v)=0.6344$

For n=4 we have: $\beta=10080$ and

where $X = z^{0.5}$ and

$$g(z) = 1 - e^{-X} \left(\frac{X^7}{5040} + \frac{X^6}{720} + \frac{X^5}{120} + \frac{X^4}{24} + \frac{X^3}{6} + \frac{X^2}{2} + X + 1 \right) \text{ where } X = z^{0.5}.$$

Here we can recognize a pattern for this functional class and it has been tested to n=5, where in general, $\beta=n(2n-1)!/2$ and the mass fraction can be written as:

$$g(z) = 1 - e^{-X} \left(\sum_{i=0}^{i=2n-1} \frac{X^i}{i!} \right); \text{ where } X = \frac{z}{z^n}.$$

Since the $i=0$ term is always 1, computationally these functions implemented in FITS.exe program with the following modification to the above:

$$g(z) = 1 - e^{-X} \left(1 + \sum_{i=1}^{i=2n-1} \frac{X^i}{i!} \right); \text{ where } X = \frac{z}{z^n}.$$

This class of functions trends to z^4 as z goes to zero a tail at large z that trails off slowly making it a good candidate to fit mass distributions that are highly peak towards $z=0$ but still need to taper off slowly.

4.1.3 When m=2

One form that has been looked at but really not used is for $m=2$ and $\alpha=1$. For this form, we have $\beta=24$ and the mass ratio function is:

$$g(z) = 1 - e^{-z} \left(\frac{z^4}{24} + \frac{z^3}{6} + \frac{z^2}{2} + z + 1 \right)$$

Note the progression of this works for $n=0, 1$ and 2 . Here this function looks like the following when plotted:

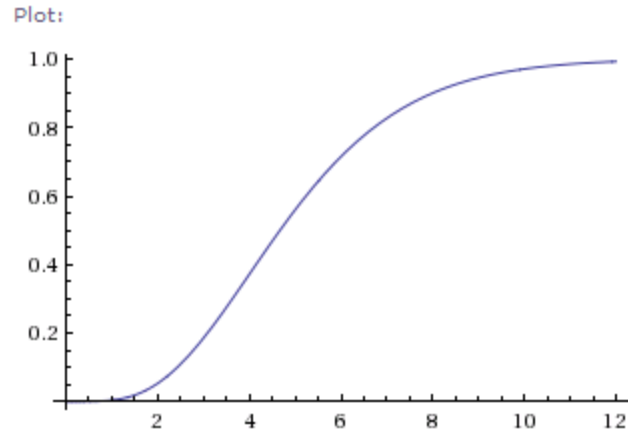


Figure 1

4.2 Functions using powers of distance

Another convenient functional form for $f(x)$ involves using powers of x as linear sums. Certain forms of these types of functions satisfy the requirements for $f(x)$. Specifically, when $f(x)$ takes on a form as:

$$f(x) = (1 - x)^n$$

Note for this type of distribution, the mass extends only to the distance where $r=a$, or $x=1$. Thus the integrals used above have their integration range limited from $r=0$ to $r=a$.

4.2.1 $F(x)=1$

The simplest of all matter distributions is the uniform distribution, or when $n=0$ above. We include this for completeness and to create it for a talking point in other discussions. In this case, $\beta=1/3$ and

$$g(z) = z^3$$

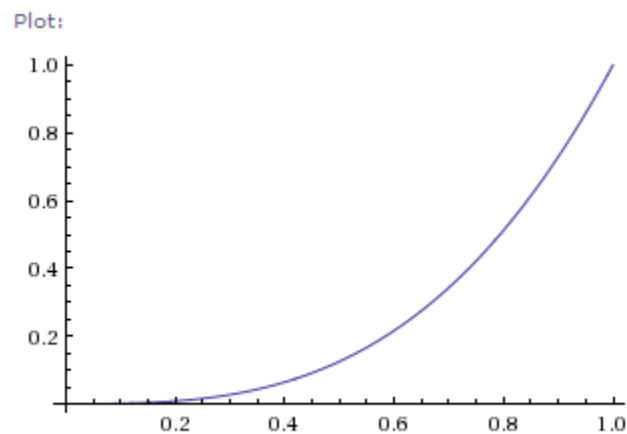


Figure 2

The $n=0$ case for uniform mass distribution is not particularly interesting and it doesn't roll off like the other distributions do as it approaches 1.

For this function, the $R_v/a=0.825$ and $g(z=R_v)=0.5819$

4.2.2 $F(x)=1-x$

The next simplest form of the above is when $n=1$.

$$f(x) = 1 - x; \text{ and } M(R) = \frac{M_T}{\beta} \int_0^{R/a} (1-x)x^2 dx$$

For this case, $\beta=1/12$ and the integral result is, again where $z=R/a$:

$$g(z) = (4 - 3z)z^3$$

The plot below shows this distribution type's behavior at $z=0$ and $z=1$. This distribution ends too abruptly and has no tail that would seem to be a necessary property. We would expect that higher orders of x will push the distribution of mass towards $x=0$.

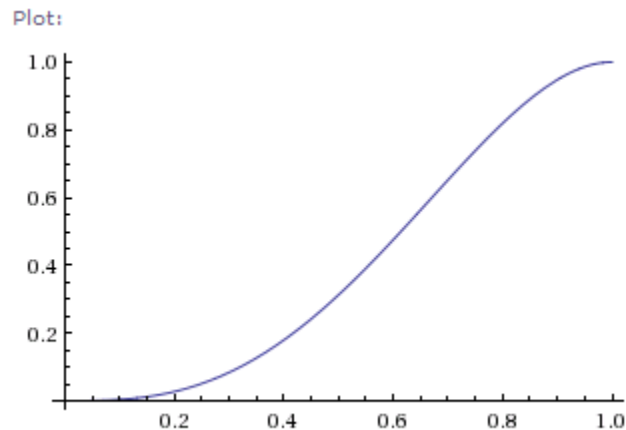


Figure 3

4.2.3 $F(x)=(1-x)^2$

For $n=2$, $\beta=1/30$ and the final integral takes the form:

$$g(z) = (6z^2 - 15z + 10)z^3$$

The plot of this function is more symmetric in z and has the property that half the mass is less than $z=0.5$.

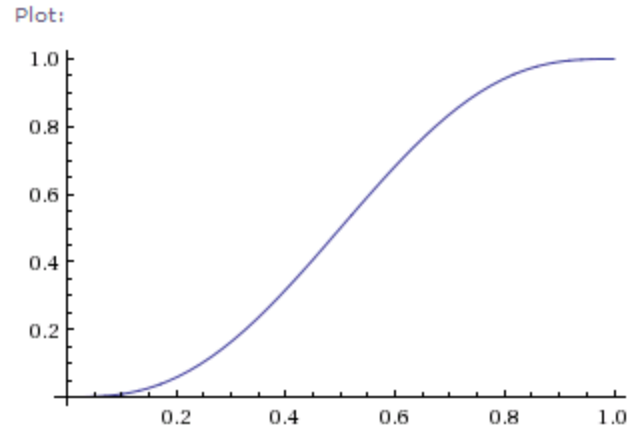


Figure 4

4.2.4 $F(x)=(1-x)^4$

Before leaving this type of function, let's look at one more, letting $n=4$. Note as n increases, the total mass is more concentrated near $z=0$. For $n=4$, $\beta=1/105$ and the mass ratio becomes:

$$g(z) = (15z^4 - 70z^3 + 126z^2 - 105z + 35)z^3$$

This mass distribution begins to look a lot like the exponential functions in its shape, least from the perspective that the distribution has a tail that extends out beyond $z=0.5$.

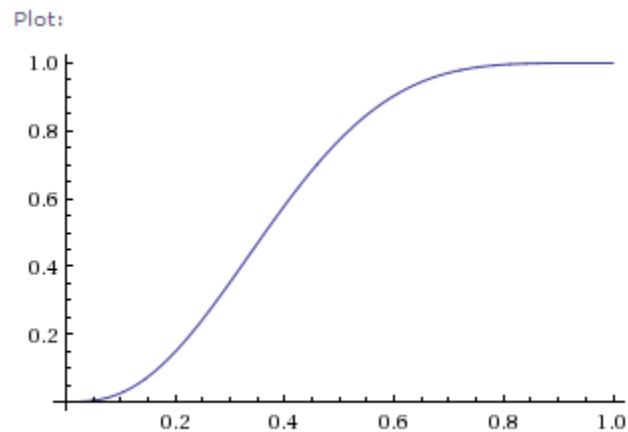


Figure 5

4.2.5 $F(x)=1-x^2$

A variation of the above $f(x)$ functions is for the following:

$$f(x) = 1 - x^2 \text{ and for this function } \beta = \frac{2}{15}$$

The mass ratio is given by:

$$g(z) = (5 - 3z^2)z^3/2$$

4.3 Other Power Law Forms

The density profiles that follow are power law functions. For compactness, we will use the following formalism to describe these functions which have the generic form:

$$F(x) = \frac{1}{x^a(1+x^b)^{p+1}}$$

For example, the NFW profile can be written as $F(a:b:p)$ with $n=1$, $m=1$ and $p=1$ or $FX(1,1,1)$. Note that a, b and p are not restricted to integers. Note that this is not how astrophysical papers parameterize these functions. I chose this method as it allows me to use the power parameter p as a variable with some of these functions to examine the effect varying p has on the density profile to replicate behaviors in simulation data.

4.3.1 FX(0:3:1)

The above form, $FX(0,3,1)$ is interesting since it is easily integrated. In this case $\beta=1/3$ and the mass ratio function is:

$$g(z) = z^3/(1+z^3)$$

The Taylor series expansion for $g(z)$ near $z=0$ is :

$$g(z) = z^3 - z^6 + z^9 - z^{12} \dots$$

Note that the z^3 behavior at $z=0$. Here is a plot of this function

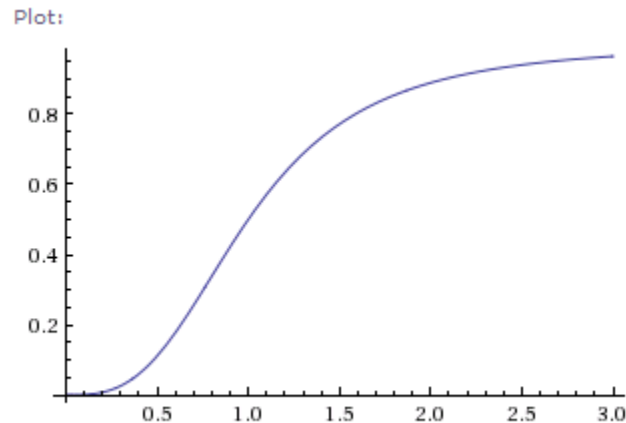


Figure 6

For this function, the $R_v/a=1.234$ and $g(z=R_v)=0.6576$

4.3.2 FX(0:3:p) (added 12/30/2013)

An interesting variation of the above form is FX(0,3,p) when a generic power of the divisor is included. This function defaults to the one in the previous section, when p=1. This function is integrable out to infinity provided that p>0. For this function, $\beta=1/(3p)$. The mass ratio is given by:

$$g(z) = 1 - \frac{1}{(1 + z^3)^p}$$

The Taylor Series expansion near z=0 for this goes as:

$$g(z) = pz^3 - 1/2(p(p + 1)z^6 + O(z^9) \dots$$

Thus, this function retains the z^3 behavior near z=0 and it has the interesting property that 1-g(z) at very large z goes as $1/z^{3p}$. This is important if one is interested in the tail properties as a function of z. My studies of gas ball distributions show that the tail of the distribution at large R follows a power law. The thought might be to use this generic distribution function, find the power law in the data and use that to help in describing distribution tail of an overall mass density distribution.

Note too that p in the above density function is not limited to integer values.

The table below gives the results of empirical results

for this distribution for various values of "p". Note that the ratio of Rv/a scales no matter for any value of "a". For example, if p=1.2 and a=45.2, the virial radius is $1.127*45.2 = 50.9$ (in whatever units one is using).

Results for a=10				
Power (p)	# Test Part.	Virial Radius	% Num for r<Rv	Rv/a
0.3	10000	20.94	63.14	2.094
0.4	10000	23.10	64.65	2.310
0.5	10000	19.44	64.38	1.944
0.6	10000	17.05	65.71	1.705
0.7	10000	15.38	65.84	1.538
0.8	10000	14.15	65.86	1.415
0.9	10000	13.19	65.83	1.319
1.0	10000	12.43	65.76	1.243
1.1	10000	11.80	65.68	1.180
1.2	10000	11.27	65.58	1.127
1.4	10000	10.43	65.41	1.043
1.5	10000	10.09	65.32	1.009
1.5	5000	10.10	65.41	1.010
1.7	5000	9.51	65.22	0.951
2.0	5000	8.84	65.02	0.884
2.2	5000	8.48	64.91	0.848
2.5	5000	8.03	64.78	0.803
2.8	5000	7.66	64.67	0.766

3.0	5000	7.45	64.60	0.745
-----	------	------	-------	-------

4.3.3 FX(-1:4:p) (added 1/8/2013)

Another interesting variant of the form in 4.3.1 is for $f(x)=x/(1+x^4)^{p+1}$, or FX(-1,4,p). This is another easily integrable function with a $\beta=1/4p$. The mass ratio function becomes:

$$g(z) = 1 - 1/(1 + z^4)^p$$

The Taylor series expansion for $g(z)$ near $z=0$ is :

$$g(z) = pz^4 + O(z^6) \dots$$

This function is interesting in that it has a large z behavior that asymptotically approaches 1 as z^{4p} . The plot of this behavior is seen below:

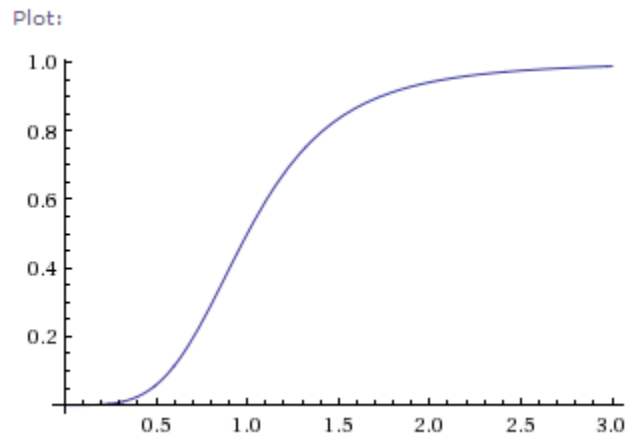


Figure 7

Note again that p in the above density function is not limited to integer values but must be great than zero. Also note, this function is tends to push out the mass contribution further from the origin than the function in 4.3.2 but the tail function can be varied to match to the power law seen in the simulation data.

4.3.4 Plummer's Model, FX(0:2:1.5) (added 3/16/2016)

I came across something referred to as Plummer's model² for mass density and potential energy for gravitating systems, FX(0,2,1.5). Plummer's model gives a full density model as the following:

$$\rho(r) = \frac{3M_T}{4\pi a^3 (1 + r^2/a^2)^{5/2}}$$

² Plummer's model is mentioned in this reference on slide 18: <http://www.maths.ed.ac.uk/~heggie/taiwan.pdf>

In the same reference, a gravitational potential energy is given as³:

$$V(r) = - \frac{GM}{(1 + r^2/a^2)^{1/2}}$$

We can see immediately that this follows the formalism of this document. We see immediately that $\beta=1/3$ without doing any integrals. The function $g(z)$ becomes:

$$g(z) = \frac{z^3}{(1 + z^2)^{3/2}}$$

For this function, the $R_v/a=1.701$ and $g(z=R_v)=0.6405$

4.3.5 General Plummer Model FX(0:p:1/p) (added 3/20/2016)

After solving Poisson's equation for the original Plummer potential and proving to myself that the potential and density functions are consistent with Poisson's equation, it occurred to me that there may be a more general form for Plummer's model. Here the Plummer shorthand is FX(0,p,1+1/p)

Suppose we pick a potential such that (Note, I have included the missing scaling factor to make the units correct):

$$V(r) = - \frac{GM}{a(1 + r^p/a^p)^{1/p}}$$

This potential reverts to Plummer's model when $p=2$. Note too that this potential has the same behavior as the usual gravitational potential for $r \gg a$, $V(r) \approx 1/r$.

Using Poisson's equation, we can determine the mass density for this potential is the following:

$$\rho(r) = \frac{M(1+p)(r/a)^{p-2}}{4\pi a^3 (1 + (r/a)^p)^{2+1/p}}$$

It can be shown that the mass density function is with $\beta=1/1+p$:

³ Note the above is directly copied from the reference and has incorrect units for a gravitational potential. Since the quantity in the denominator above is unit less and we need to divide the above by a distance, I suspect that this can be corrected with the following change (Note, Wikipedia confirms this on its page for the Plummer Model https://en.wikipedia.org/wiki/Plummer_model :

$$V(r) = - \frac{GM}{a(1 + r^2/a^2)^{1/2}}$$

I have now have tried the math and for this potential and density, it is an exact solution of the Poisson equation.

$$g(z) = \frac{z^{p+1}}{(1+z^p)^{1+1/p}}$$

After doing some study in this function, it may have some uses for $p \leq 3$, but beyond that, mass becomes strongly concentrated near the scaling parameter “a”. In addition, the $p=2$ solution is the only one which has $g(z) \approx z^3$ near $z=0$. This last property seems important because at least empirically speaking, my simulations always seem to demonstrate a near uniform mass distribution near the origin.

4.3.6 NFW(M) Density Profile: FX(1:1:1) (added 8/24/2018)

A common profile used in the astrophysical literature is the Navarro, Frenk, White⁴ (NFW) profile (FX(1,1,1)). I have avoided adding this as discussion as it is function that its integral does not converge at infinity. As such, in the literature, they only integrate out to a large distance. For my purposes, I integrate out to when a large, maximum distance R_m and $x_m = R_m/a$. As such, I will refer to the NFW profile as NFW(M) where the M stands for the maximum distance for the integral. It can be shown that:

$$\beta_m = \log(1 + x_m) - x_m/(x_m + 1)$$

And

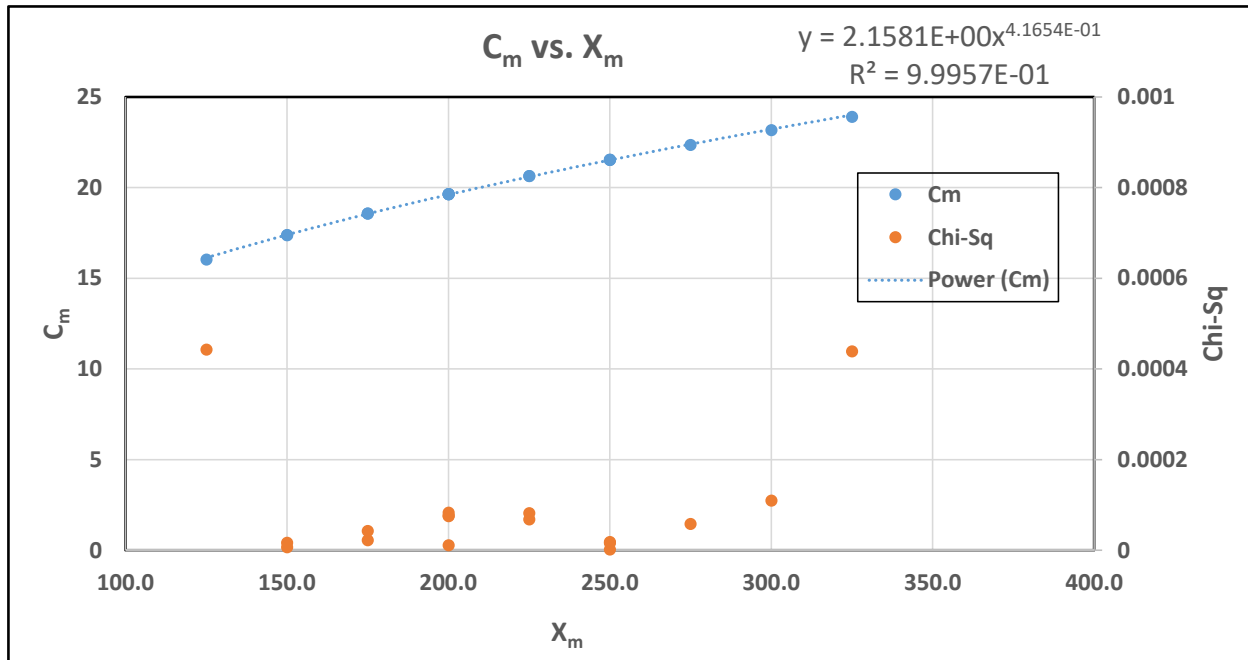
$$g(z) = \left\{ \log(z + 1) - \frac{z}{z + 1} \right\} / \beta_m$$

For this function, I have determined empirically that for $X_m=200$, $R_v/a=19.65$ and $g(z=R_v)=0.4817$ (verified 10/19/2020).

The above relationship between the virial radius and the NFW(200) profile is seen throughout the included density profiles. However, the values of C change with the maximum integration distance, R_m and consequently X_m . For all the density profiles herein except the NFW profile we can define a constant that shows the direct relationship between the virial radius and the profile scaling constant. As we have seen previously, $R_v/a=C$. For the NFW profile, C and the resulting scaling constant are dependent on the choice of X_m . Thus, for the NFW profile, I write this as $R_v/a_m=C_m$.

I created a test group of NFW profiles with differing X_m values and in many cases several examples of the same X_m . In each case the NFW scaling length was set to 1 in whatever units one chooses. After the distribution was created, the virial radius was computed and since $a=1$, $R_v=C_m$. This data is presented below along with the Chi-Square comparison with the data and the power law:

⁴ Navarro, J.F., Frenk, C.S., & White, S.D.M. 1995b, MNRAS, 275, 56



Some notes on the above data. Each distribution was created with 50,000 particles. Distance units are irrelevant and can be the choice of the user; X_m and C_m are unitless.

We can see from the power law fit that the C_m and X_m relation is good. A number of data points outside these X_m values were included initially in this analysis but were deemed too far outside bounds of normal usability and thus removed from the fitted set of data above.

The best way to use this information when doing density profiles of gravitating systems, us to pick a X_m (200 works for a start) and then calculate the C_m using the power law above. Divide the calculated virial radius by the C_m and this will be the NFW scaling distance for that X_m . Checking the elbow in the phase space plot will give an indication of the maximum radius and that can feed back into picking a more appropriate X_m , iterate are needed.

4.3.6.1 Practical Solution for Scaling Constant from Simulation Density Profile

Using the NFW profile is problematic in that the profile's normalization, β is highly dependent on the maximum distance that one integrates out to. In addition, creation of NFW density profiles shows that the virial radius increases significantly with increasing maximum distance. As such, the method used for the NFW-200 ($R_{\max}=200a$) does not always provide a solution for the scaling that represents the best representation for the simulation profile results.

The following method was developed to improve the overall extraction of the scaling constant. Starting with the profile, it was recognized that using the simulation profile data one could extract the scaling constant. Begin with the profile at any point for the NFW density function is the following:

$$\rho(r) = \frac{M_T}{4\pi a^3 \beta} \frac{1}{x(1+x)^2}; x = r/a$$

For any two points in the profile, one a minimum point R_0 and then some arbitrary point greater than the minimum R , the theoretical ratio of the densities for these two points can be written:

$$\frac{\rho_0}{\rho} = \frac{R(a + R)^2}{R_0(a + R_0)^2}$$

Which has the solution:

$$a = \frac{R - kR_0}{k - 1}; \text{ Where } k = \sqrt{\frac{\rho_0 R_0}{\rho R}}$$

Once the scaling constant is known, the product of the total mass and β can be determined and if one uses the full total mass, then β can be also determined. Note that $k=1$ for $R=R_0$ and increases with increasing R .

Implementing this solution in an analysis spreadsheet is a bit more awkward than just putting two distinct points on the distribution into the above solution. The density profile is highly variable from point to point and thus the solution will be as variable. To mitigate this variability, the density profile is “averaged” using the fact that the density profile in a log-log plot is linear overall in segments. A linear regression of the log data provides a “average” density at the point of interest based on neighboring points in the profile. This is done for all points between limits based on the measured virial radius. The average of all the scaling range solutions are then used as the final scaling length.

In practice the above method produces good results. One must be mindful of the limits chosen in the spreadsheet, specifically the lower limit should be chosen to be greater than the point in the profile where the density flattens. The sensitivity to the upper limit is less and one can play with both limits to see how the result is affected. Note too that the standard deviation of the scaling length solution can be as high as 30% of the average value, indicating the solution is also not without some uncertainty.

4.3.7 Jaffe Profile (Extended) : FX(2,1,p) (added 8/24/2018)

Another profile I have found in the literature is the Jaffe profile⁵, FX(2,1,p). I have made a more generic version below, where $p=1$ is the Jaffe form. I find this extended version of the Jaffe profile interesting in that it can be used to fit the outer portions of simulation data for force-softened simulations. Since this profile has an integrable form to infinity, $\beta=1/p$. The mass ratio for this function is:

$$g(z) = 1 - \frac{1}{(1+z)^p}$$

Note that this profile is highly cusped towards the inner portions of the distribution. It is also a profile that has the behavior ($r < a$; $g(z) \rightarrow z$) which coincidentally can contribute to the flattened rotation curves seen in galaxies.

⁵ I was investigating the extended form before I even knew that the $p=1$ form was associated with Jaffe. I have given proper credit here as a result.

For $p=1$, $R_v/a=1.058$ and $g(r=R_v)=0.5214$ (verified 10/19/2020)

4.3.8 FX(1.5,1,1) (added 11/26/2022)

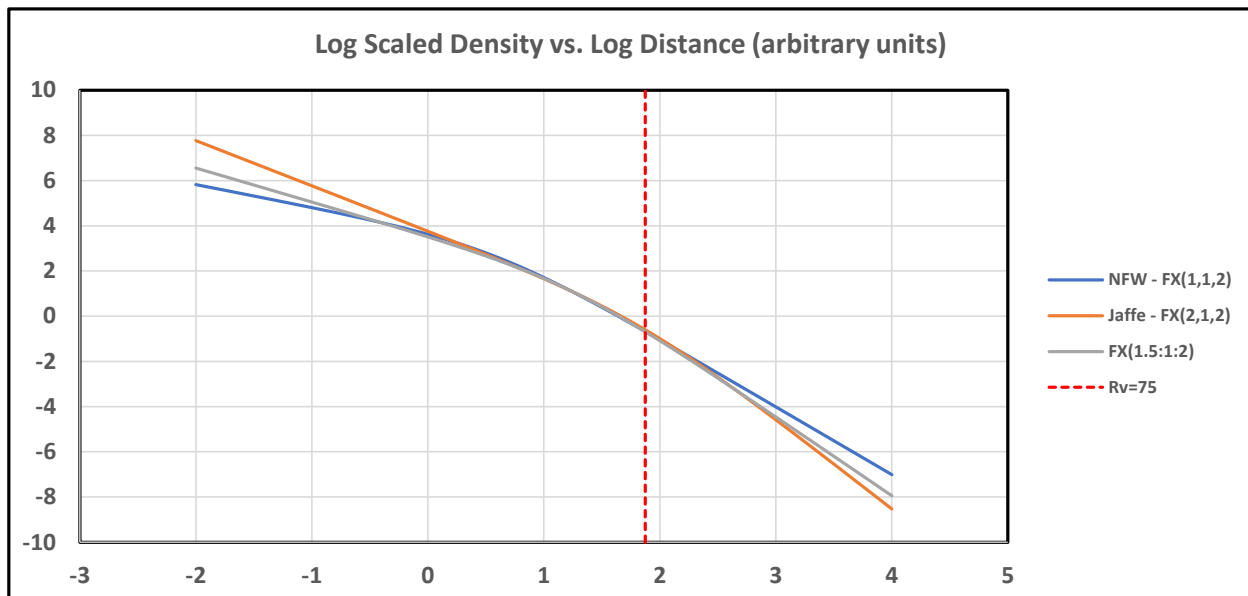
I began investigating this function recently as a go-between the NFW and Jaffe profiles. Since both of those known profiles are interesting when comparing simulation results, I thought that perhaps this function might be of interest since it has well behaved $M(R)$ integral out to infinity.

For this function, the mass ratio is:

$$g(z) = \tan^{-1}(\sqrt{z}) - \frac{\sqrt{z}}{1+z},$$

with $\beta=\pi/2$ and $R_v/a=4.222\pm 0.002$. The latter number determined empirically by creating 39 distributions with 90,000 particles. The uncertainty was the standard deviation in R_v of the 39 distributions.

The figure below compares the NFW, Jaffe and the FX(1.5:1:1) density profiles. Noteworthy is that at the profiles extremes, the FX(1.5:1:1) profile does indeed come between the NFW and Jaffe profiles as one might expect given the similarities of these profile definitions.



5 Notes on Using the Density Functions

For my own reference, I include here a quick discussion on using some aspects of the formalism presented here.

5.1 Comparing Simulation Data to the Density Model

Equation 8 gives a very straight forward and easy use of the $g(z)$ functions. Data from my simulation, cast as the quantity $M(R)/M_t$ can be directly compared and "fit" to distribution functions as seen in previous documents. However, reconstructing the density functions from these analytic expressions can

be somewhat misleading. Because these density functions only depend on the radius, and since the integral is a three dimensional integral, the radial dependence of the mass density function is muted or obscured at large distances.

What that means is the mass contribution of the density function is weighted more heavily to $r=0$ than to the large r component. Comparing density functions for different functional types can obscure the mass contributions at large r . Figure 8 illustrates this effect. The density function for several different $f(r/a)$ is plotted where each density function was scaled such that 50% of the total mass is at $r=2$. I used the definitions above from where the density function is written (remember that $x=r/a$):

$$\rho_i(r) = \frac{M_{Ti}}{4\pi a_i^3 \beta_i} f_i(r) = \frac{M_{Ti}}{4\pi a_i^3 \beta_i} f_i(x)$$

The plots in Figure 8 are the exact density functions for an arbitrary total mass $M=1$. It is not obvious looking at this plot that for each function, that half of all the mass is within a radius of $r=2$ and that the other half of the total mass is beyond $r=2$.

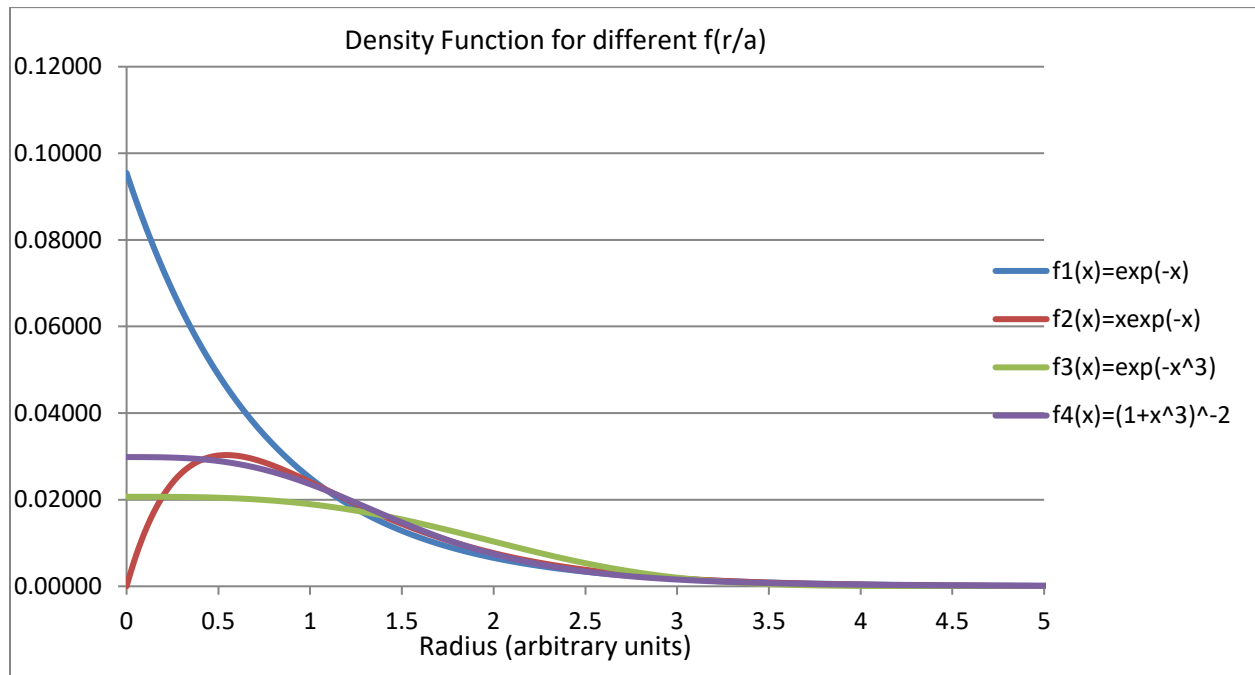


Figure 8

A better technique to evaluate these density functions and their mass contributions at distance is to look at the “area under the integrand curve” for the differing functions. Comparing them together, one can get an idea of the relative contributions at different values of r . Combining Equation 2 with the density function above and performing the angular integrals, we arrive at a integrand function, $h_i(r)$ such that:

$$M_i(R) = \int_0^R \rho_i(r) d^3r = \int_0^R h_i(r) dr$$

And of course $h_i(r)$ is defined as:

$$h_i(r) = \frac{M_{Ti}}{a_i^3 \beta_i} r^2 f_i(r) = \frac{M_{Ti}}{a_i \beta_i} x^2 f_i(x)$$

Figure 9 shows the radial component of four density function integrands. The density functions are again scaled such that 50% of the total mass is at $r=2$, as in Figure 8.

For the same total mass, the integrand curves, $h(x)$ for each of the $f(x)$ illustrates using $h(x)$ comparison makes it clearer that the area under each curve looks approximately the same. However, when constructing the density function alone, the mass contribution at large r is obscured.

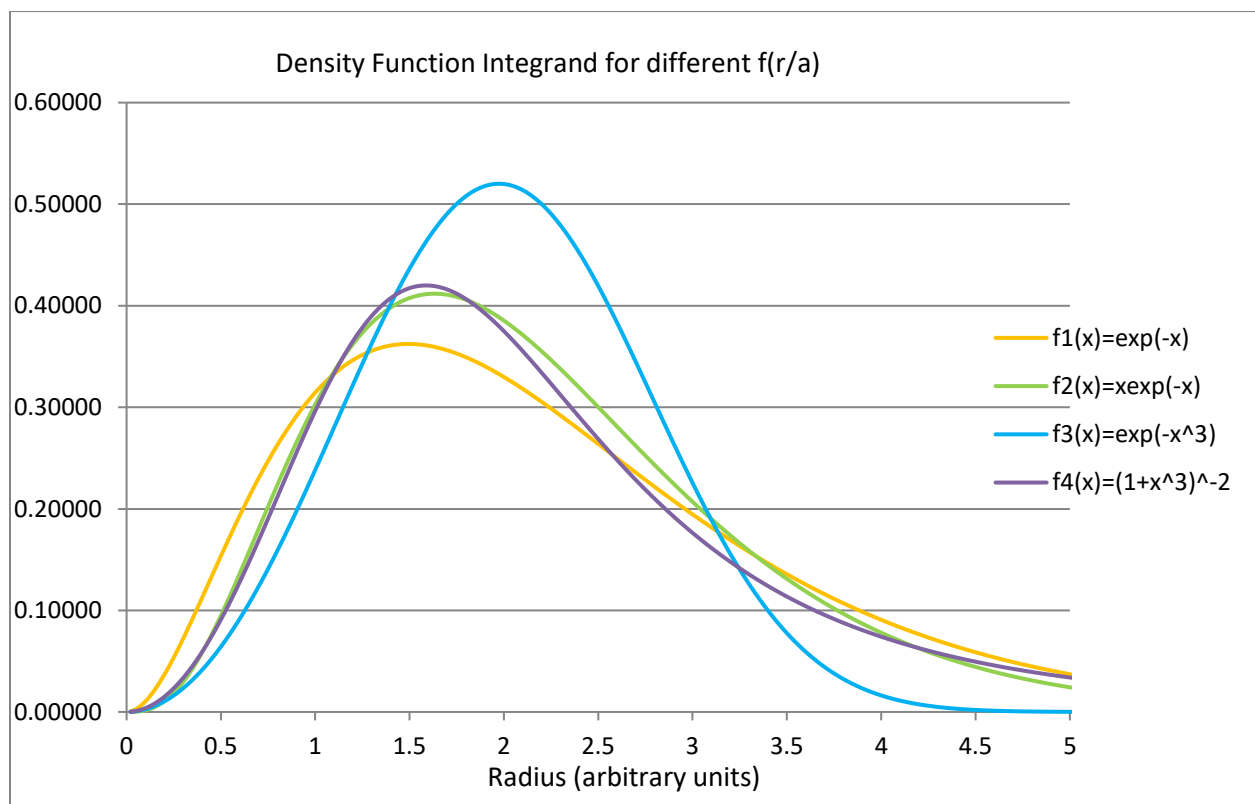


Figure 9

5.2 Reconstructing the Density Function from the Mass Function

One more observation in the above analysis is important for analysis of density functions from simulation data⁶. The following equation from above can be recast to compare with simulation data, the total mass at distance is:

$$M(r) = \int \rho(r) d^3r = \int \rho(r) (4\pi r^2) dr$$

Or

$$\frac{d}{dr} M(r) = 4\pi r^2 \rho(r)$$

And finally

$$\rho(r) = \frac{1}{4\pi r^2} \frac{d}{dr} M(r) = \frac{1}{4\pi r^2} \frac{\Delta M(r)}{\Delta r}$$

The final factors in the above equation can be extracted directly from simulation data. The derivative of the mass function can be used to extract the simulation density at any given time epoch. Note that in the above equation, $\rho(r)$ has units of mass per unit volume as a mass density should.

5.3 Poisson Equation and the relation between the Density and M(R) (Added 2/24/2017)

I lay awake one recent morning thinking about the Poisson equation and how to relate the force on an object inside a spherical mass density. I noted some simplifications provided you want to utilize force concepts rather than gravitational potentials. We all know the Poisson equation for the gravitational potential is the following:

$$\nabla^2 \phi(r) = 4\pi G \rho(r)$$

Since the potential ϕ is only dependent on the radius, we can write out the ∇^2 operator explicitly in the above equation:

$$\frac{1}{r^2} \frac{\partial}{\partial r} \left[r^2 \frac{\partial}{\partial r} \phi \right] = 4\pi G \rho(r)$$

I was actually thinking about the above form and how the derivative of ϕ in the above is related to the force on a particle of mass “m” by the following:

⁶ I am embarrassed to mention that the main reason for including this section is that I spent about two weeks (real time working on and off) trying to figure out the above relationship. While, my simulation-analysis spreadsheets show perfect correlation between the integrand method in the previous section, I could not quite figure out what I needed to do to extract the density function from the simulation M(R). What I was missing was the above 4π and not getting units correct in the spreadsheet calculation of the derivative (M(R) slope).

$$\vec{F}(r) = -m\vec{\nabla} \phi(r) = -m \frac{\partial}{\partial r} \phi(r) \hat{r}$$

Dropping the vector notation since the magnitude of the distance “ r ” is all that matters in this case we can write this as:

$$-F(r)/m = \frac{\partial}{\partial r} \phi(r)$$

Note that we now can plunk the left hand side of the above equation into the radial Poisson equation up top to get the following:

$$\frac{1}{r^2} \frac{\partial}{\partial r} \left[r^2 \left(-\frac{F(r)}{m} \right) \right] = 4\pi G\rho(r)$$

Or

$$\frac{1}{r^2} \frac{\partial}{\partial r} [r^2 F(r)] = -4\pi m G\rho(r)$$

We can write the radial form of the force as the following, noting that the mass of the distribution is really modified by the mass of the interior portion of the distribution of $\rho(r)$. In this document I have written this mass portion as $M(r)$ and so we have:

$$F(r) = -\frac{GmM}{r^2} = -\frac{GmM(r)}{r^2}$$

Using the above to further our Poisson extraction to get:

$$\frac{1}{r^2} \frac{\partial}{\partial r} \left[r^2 \left(-\frac{GmM(r)}{r^2} \right) \right] = -4\pi m G\rho(r)$$

Reducing this by dividing out the “ $-mG$ ” and r^2 terms we get:

$$\frac{1}{r^2} \frac{\partial}{\partial r} M(r) = 4\pi\rho(r)$$

Or

$$\rho(r) = \frac{1}{4\pi r^2} \frac{\partial}{\partial r} M(r)$$

Note that this is the exact result we arrived at in the previous section. However, that result was one I arrived at from trying to extract the density from my simulation data histograms. This result came from thinking about how modified forces via an $M(r)$ function would manifest in the density function.

Using this result, one can test analytical $M(r)$ variants and easily determine the density function and its extrema conditions ($r \rightarrow 0$ and $r \rightarrow \infty$). These extrema are of high interest in the literature discussions of Dark Matter Halos and are partially why I am interested in using this result.

6 Using This Formalism (Added 5/15/2016)

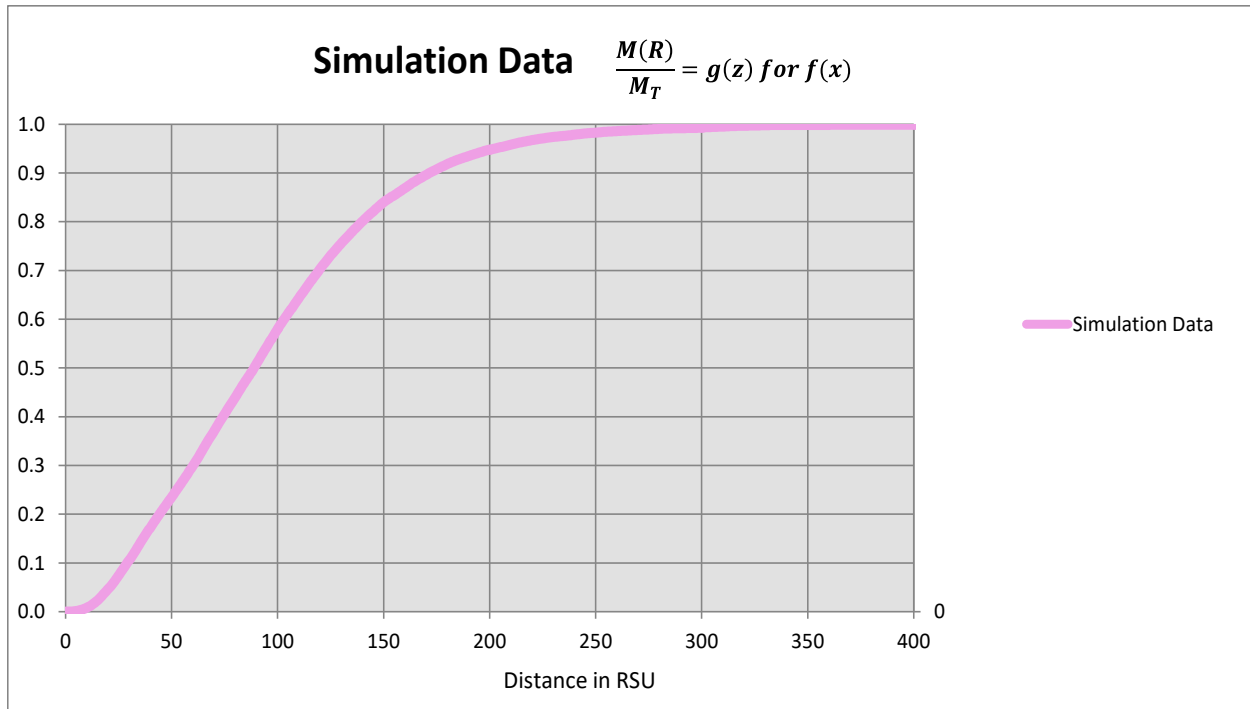
In this section, I will document how I use the above formalism to extract mass distribution parameters from the data obtained from my gravitational simulation. I have an ongoing study that I am looking at how a collection of “small” masses evolve over time. Here is some of what I do with this simulation data and how I analyze its behaviors.

6.1 About the Simulation Data

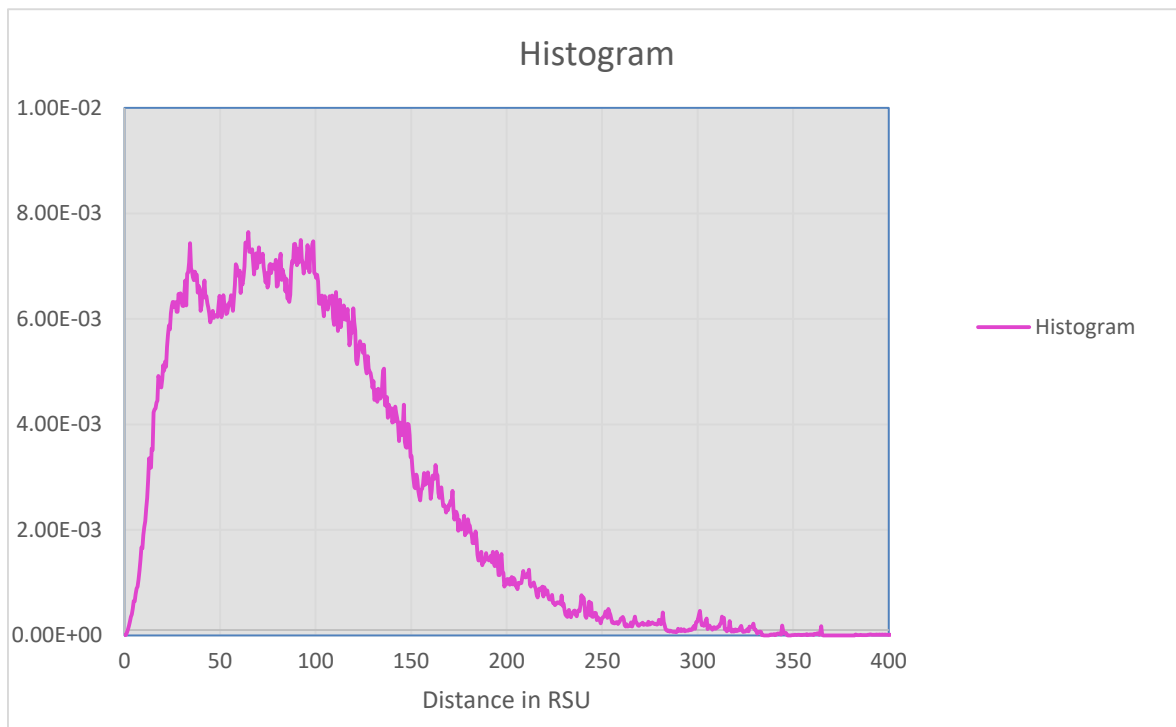
The simulation pumps out at regular intervals position files that are saved in the simulation computer’s disk drive. One can read through these data files and extract a distribution of the mass at distance. I have a standalone program that extracts this information and after some corrections for movement of the center of mass, extracts a distribution of mass. A file is created for this histogram that can be exported easily into a spreadsheet. The contents of the file look like the following:

Bin	Radial Distance	Number of Mass Particles	Integrated Sum of Masses
0420	1001	5	5
0	0.2500	5	5
1	0.7500	20	25
2	1.2500	88	113
3	1.7500	170	283
4	2.2500	271	554
5	2.7500	394	948
6	3.2500	527	1475
7	3.7500	604	2079
8	4.2500	759	2838
9	4.7500	977	3815
10	5.2500	968	4783
11	5.7500	1181	5964
12	6.2500	1339	7303
13	6.7500	1394	8697
14	7.2500	1592	10289
15	7.7500	1843	12132
16	8.2500	2146	14278
17	8.7500	2506	16784
18	9.2500	2483	19267

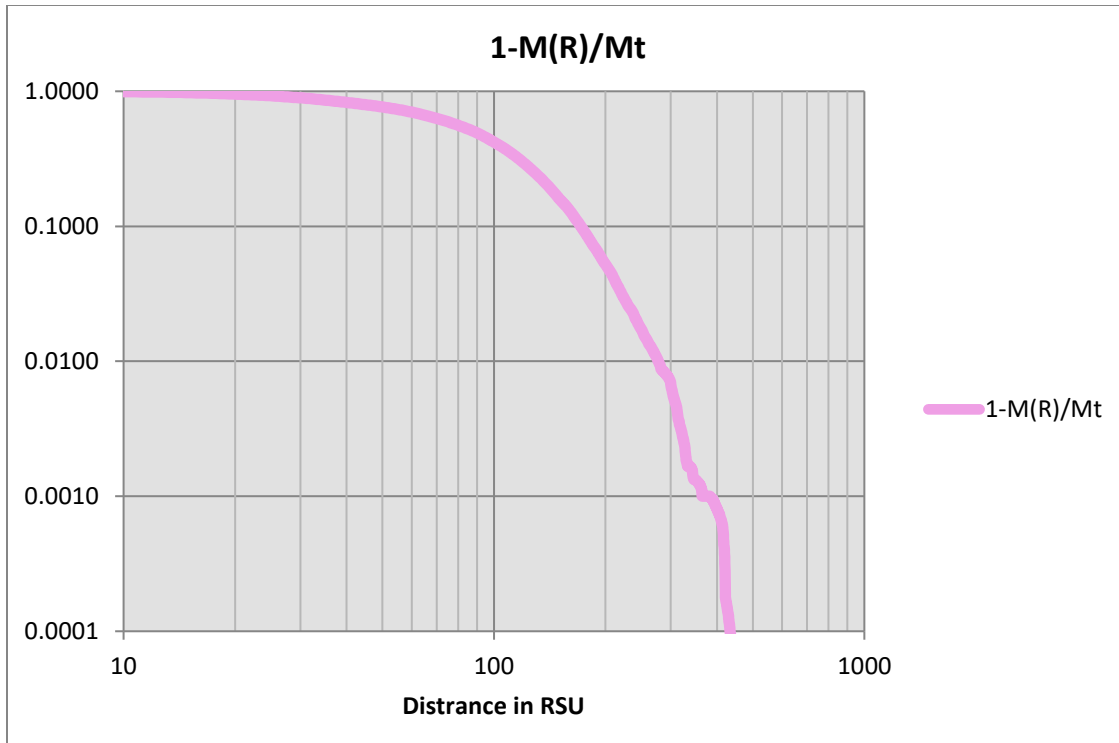
In the above example, there are 3000 objects in the simulation and 1001 files are read in, skipping every 5 files, and then masses are binned in 5/10 simulation units bins (I will use the acronym RSU, RIOD Simulation Units to refer to the unit system used in the simulation). The information across the lines is, the bin number, the radial distance for the bin, the number of mass particles in that bin and finally the integrated sum of the masses, respectively. The mass distribution and the integrated sum produce plots that show the distributed character of the mass. For example, the following plot is the ratio $M(R)/M_T$ for the above data. This is a typical mass ratio plot for these types of simulations. Empirically, it has been seen that the mass ratio will evolve with time with the small r behavior pulling in tighter and the large r behavior flattening out.



For the above data, the mass at distance distribution looks like the following:



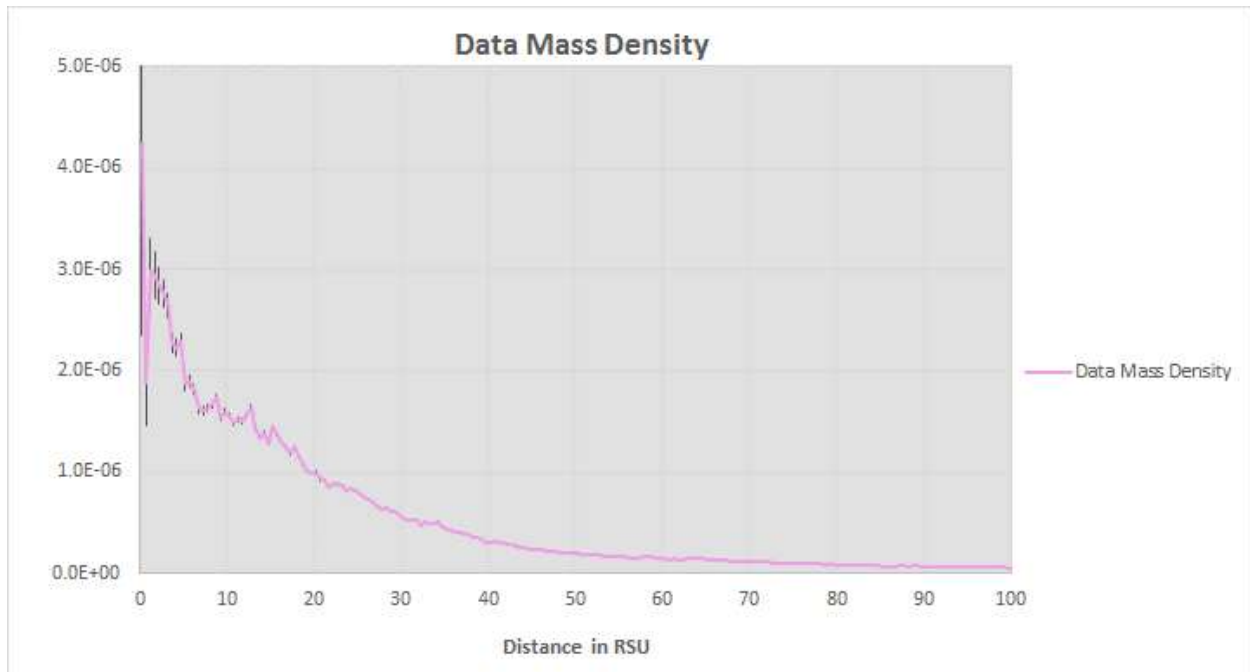
Please note that above histogram when integrated (summed) produces the $M(R)$ plot immediately above it. Another interesting view of this data is when one plots the following $1 - M(R)/M_T$, shown below:



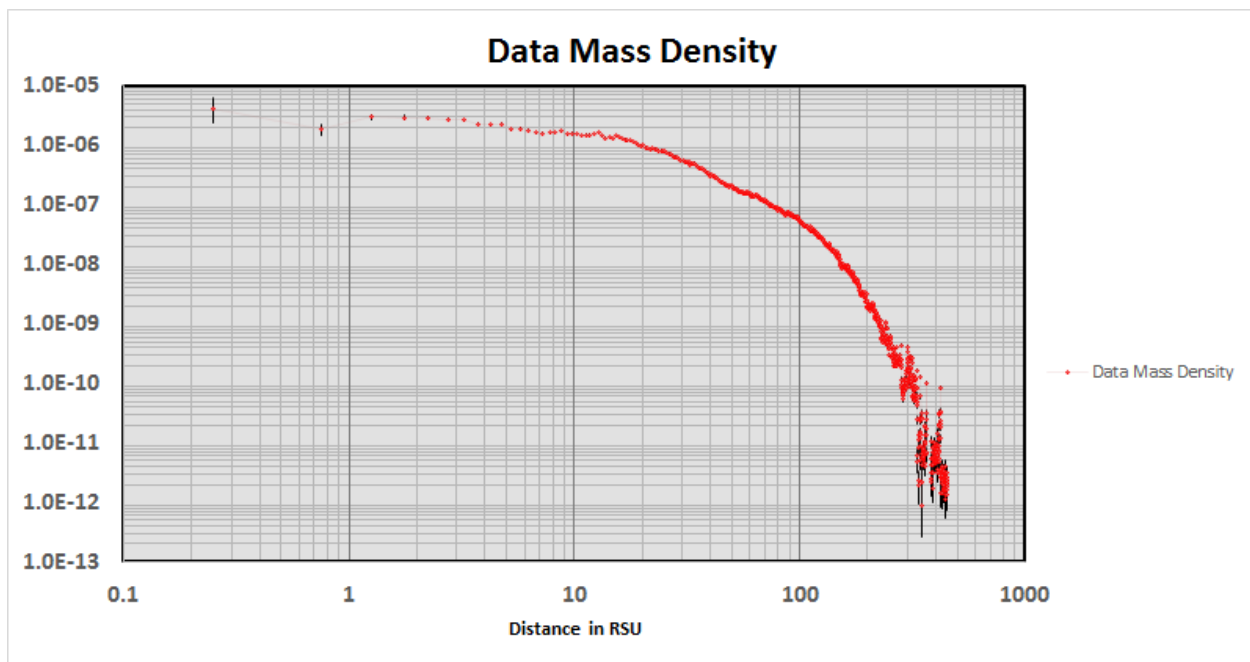
This plot demonstrates the behavior at large distances and (and it is not as noticeable in the above example) for large distances, many of these type of plots show a strong linear behavior in this presentation. What that usually means is that underlying behavior is a power law and extracting that power law can reveal some inherent property of these evolving systems. In light of the above perceived power law, I could pick one of my mass distribution functions as one which exhibits a power law behavior.

Finally, one can extract the overall mass density function from the above data using what was presented in Section 5.2. The first of two plots below is straight linear representation of mass density data. Note that the units system here are still RSU.

In this particular view what is important is the behavior near $R=0$. In this example there appears to be a strong peak near the origin. However, in this region the data is not as statistically significant as noted by the large uncertainties plotted with data and thus drawing conclusions of a real peak is premature.



The next plot shows log-log plot of the extracted mass density. This time no line is drawn between points to emphasize the behavior at distance.



Looking at the above plot, three fairly distinct regions of behavior are exhibited. First, from about 10 RSU inward, this resembles very flat behavior and could be construed to be a “uniform-like” distribution. Secondly, from about 25-120 RSU is a region where there seems to be uniform decrease in the mass density. Finally from about 200 RSU and above there is a stronger fall off of the mass density; a

significantly steeper behavior than the middle section. This same three part behavior is observed in nearly all the mass distributions analyzed from the simulation.

6.2 Modeling the Mass Distribution Data

The formalism defined in Section 3 of this document was designed to help model mass distributions. The observed behavior regions noted in the previous section played a role in creating this superposition mass distribution formalism and is thus used to find a few-parameter model for the distribution.

The model chosen for the mass distribution is a superposition of three mass density functions. There are many different functions presented within this document to choose from as model constituents. Picking appropriate functions and then finding the appropriate parameters to “fit” the data is the ultimate goal of this exercise. For this example, three distribution functions were selected to comprise the density model. Those three functions are as follows:

$$f_1(x) = e^{-x^{3/2}}; \text{ Discussed in Section } \textbf{Error! Reference source not found.}$$

$$f_2(x) = xe^{-x}; \text{ Discussed in Section } \textbf{Error! Reference source not found.}$$

$$f_3(x) = x/(1 + x^4)^{p+1}; \text{ Discussed in Section 4.3.3}$$

Note remember that for each $f_i(x) = f_i(x_i) = f_i(\frac{r}{a_i})$ where a_i is the range scaling factor.

Each of these functions were chosen because their behaviors closely match the three segments observed in the density data. For this model, there are 6 free parameters, three radial scaling factors, two mass contribution fractions and the exponent “p” in f_3 . Note that the mass contribution fractions are constrained to add to unity, so once two values are set, the third is determined. In practice, there are only five free parameters because the value of “p” can be directly determined from the slope of the data.

The other important aspect of this process is the $M(R)/M_T$ data is what is actually fit to the model. Each of the density functions has a direct mass ratio function as defined in the above formalism. The mass ratio is a well-behaved function, monotonically increasing from 0 to 1 and thus is ideal for fitting. Once that fit is obtained the density model is easily determined.

The fit for the mass ratio is done by a crawl through “Chi-Square” space to determine the best parameter fit to the simulation data mass ratio function. Another standalone program performs the chi-square space crawl. One chooses the function and a range and step size for each of the parameters and a best fit is generated based on a minimum chi-square. Additional iterations of this process are generally required in order to refine the fit and to approach diminishing returns on the parameters.

6.3 Mass Density Analysis Results

For the above data example, I will include the results of one such full model analysis. The data in this example is from a part of a simulation run which is in its early phases of evolution and thus the data

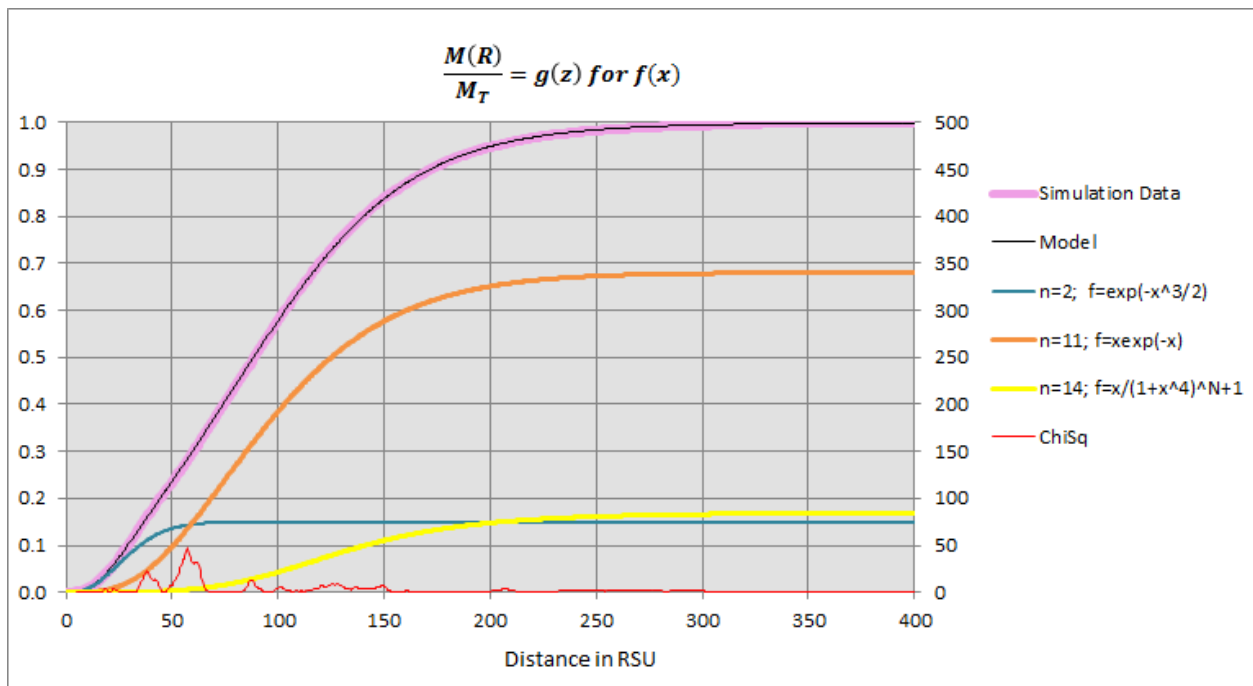
extracted at this time point in the evolution is still quite immature. However, this analysis method works well for most of the mass ratio shapes that are encountered.

The table below gives the final extracted parameters for the model fit. Note all units are RSU.

Function	Mass Ratio Contribution $M(R)/M_{T1}$	Distance Scale (a_i)	Notes:
$f_1(x) = e^{-x^{3/2}}$	0.150 ± 0.005	20.0 ± 0.3	This function was chosen because of its strong, flattened peak near $r=0$. It is also the only function in this example that has the behavior of $f(x) \rightarrow r^3$ near $r=0$
$f_2(x) = xe^{-x}$	0.680 ± 0.005	25.0 ± 0.3	This function is chosen to be the connector between the origin and large r behaviors. Note that this function behaves $f(x) \rightarrow r^4$ near $r=0$, pushing the mass associated with it out farther in distance.
$f_3(x) = x/(1+x^4)^{p+1}$	0.170 ± 0.005	138.0 ± 0.5	This function has the same behavior as the above function near the origin but also produces a power law at large distances, extracting $p = 1.2$ from the fit.

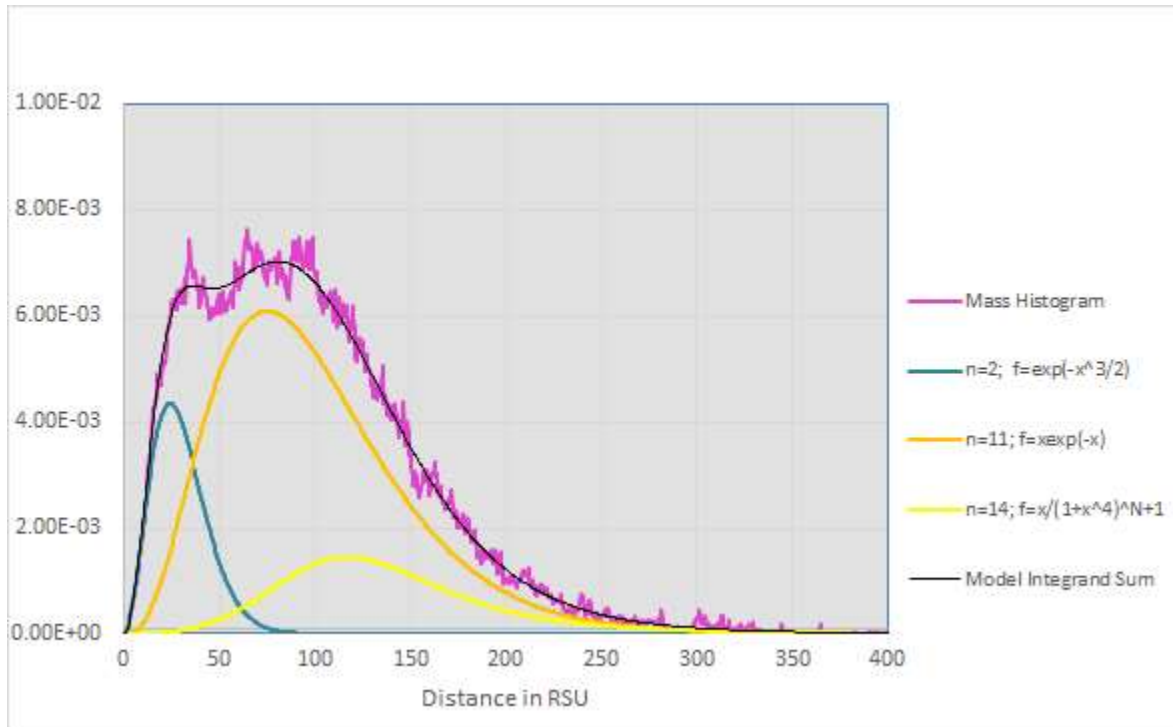
Note: The uncertainty of these measures are estimated by the taking half of the final step size in the chi-square space search. For example, the smallest step size for the mass ratio was 0.01, so the uncertainty of the measure I estimate to be half that, or 0.005.

This fit produces the following plot for the mass fraction function:

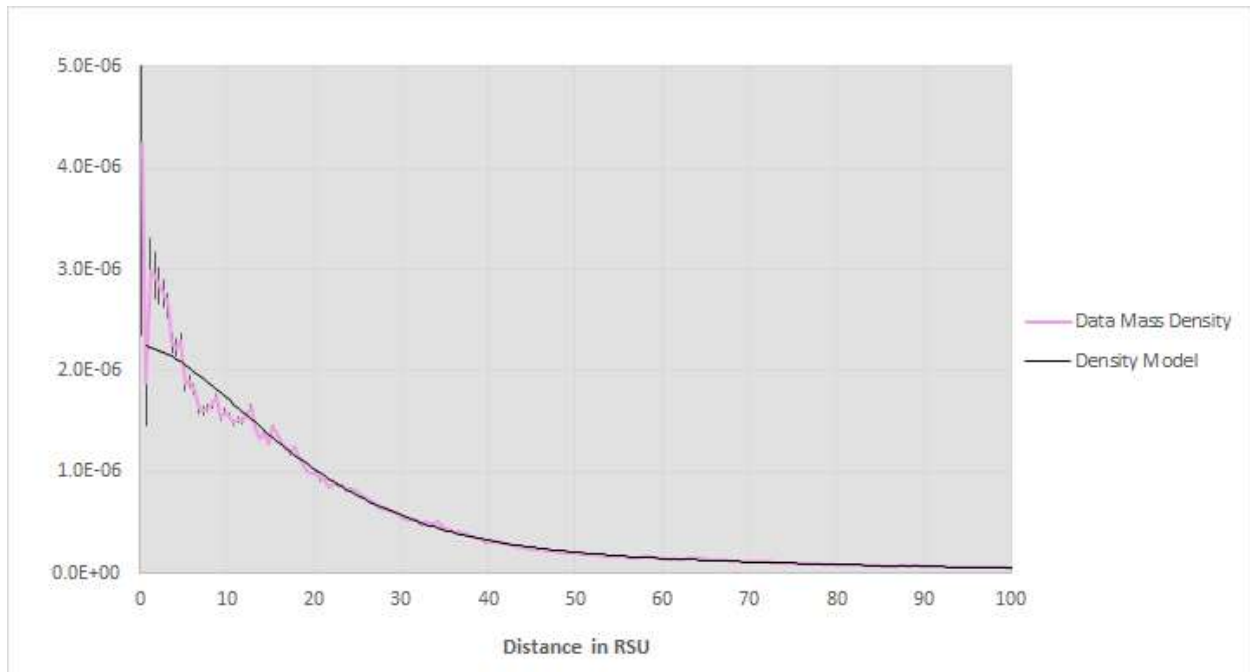


In this plot the data again is represented by the thick pink line, the data model is the thin black line which pretty much falls right on top of the data. Note that also present are the three individual density functions and their contribution to the total model density. The contribution to the Chi-Square sum is also represented in this graph and is an indication where the model deviates from the data.

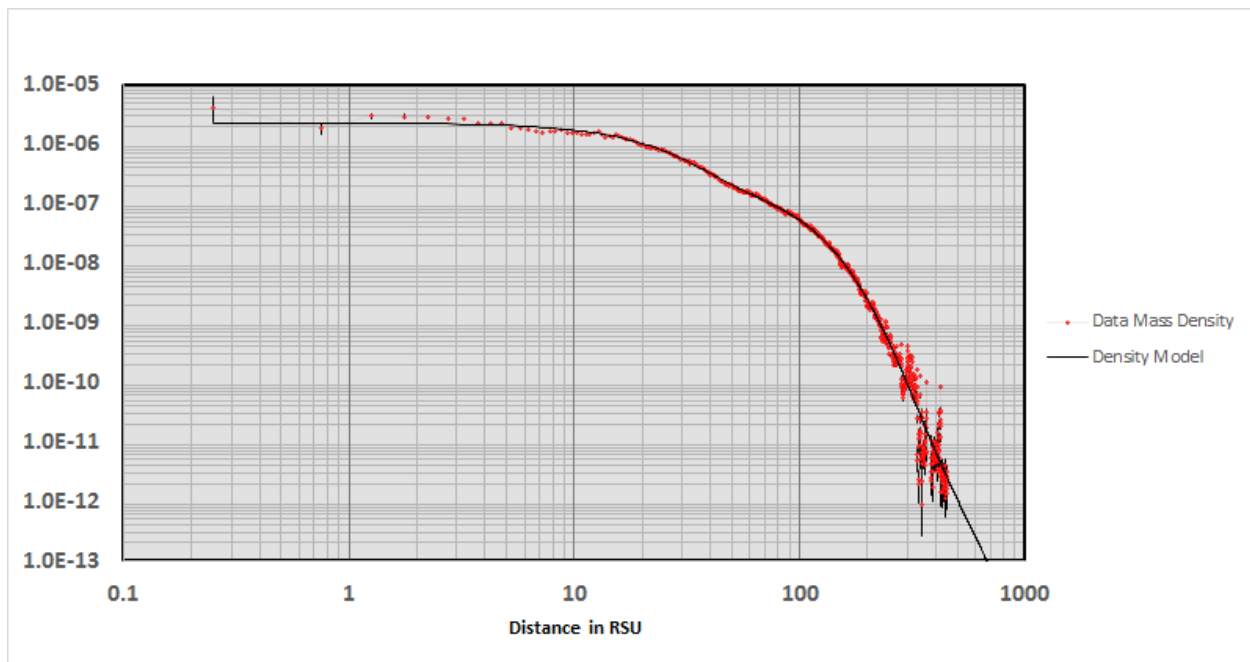
Below is the mass histogram shown with the contribution from each of these functions. It is a “happy” coincidence that the double hump at the peak of the distribution is “matched” by the model in some way.



The resulting mass distribution appears in the next two plots as shown before. Note that now the density model is overlaid on the data. The model does a respectable job representing the data beyond about 25 RSU. The observed peak at less than 5 RSU is not well represented but that is expected since the fit model had no way of resolving that scale of detail.



The final plot is the log-log plot with the density function overlaid on top of the density data. Here we see that the model does a creditable job of representing the data throughout the various segments previously discussed.



Physicists are fond of saying that you can fit anything given enough free parameters and this exercise will do nothing to dispel that notion. However, the model was chosen based on the character of the data and one can see how each of the pieces contributes to the final model. In essence, this method is fairly straight forward and simple (it would have to be since I came up with it). The results are interesting

because the important parts of these mass distributions are the near and far end behaviors. Near $r=0$, the mass distribution resembles a uniform distribution and for large r , there appears to be a power law driving the behavior. This is seen in the density analysis for many different simulations.

7 Conclusions

I have presented formalism for using spherically symmetric mass distributions. I have also presented a sampling of distribution candidates for use in my simulation code. I have presented for my own reference, how to ultimately extract mass density functions from simulation data that can be compared to a density model using the included formalism. Finally, I have presented the method for using this formalism to extract a mass density model from my simulations.

The studied distributions are all interesting candidates for mass distributions in the simulation. However, distributions that have behaviors that go as R^3 near $R=0$ are probably best suited for modeling behaviors near $R=0$. We have seen that the exponential function is the most promising and useful of the group. The functions in Section 4.3.1 and Section 4.3.2 are interesting in that they have the desired R^3 behavior near the origin. However, the behavior at large R can be tuned using a variable exponent as seen in Section 4.3.2.

The original intent of this study was to examine how these distributions might be used in the simulation. However, I have not decided exactly how to utilize the distributions in that regard. One variation is using these distributions in my code for modifying object behaviors when they get close enough for their radii to overlap. Currently, I do use the function in Section **Error! Reference source not found.** to modify forces when objects get close in the simulation. That discussion can be found in the simulation User Guide. I may discuss further uses of the discussed mass density formalism in a separate document in the future.